

# Raman spectroscopic image analysis on micropatterned graphene

Wooseok Choi<sup>1</sup>, Joonkyu Park<sup>1</sup>, Jongwan Jung<sup>1</sup>, Yongho Seo<sup>1</sup>, Jinho Ahn<sup>2</sup>, In-Sung Park<sup>2</sup>

<sup>1</sup>Faculty of Nanotechnology and Advanced Material Engineering, GRI, and HMC, Sejong University, Seoul 143-747, Republic of Korea

<sup>2</sup>Institute of Nano Science and Technology, Department of Materials Science and Engineering, Hanyang University, Seoul 133-791, Republic of Korea

E-mail: yseo@sejong.ac.kr

Published in Micro & Nano Letters; Received on 20th March 2013; Revised on 29th April 2013; Accepted on 1st May 2013

A study has been conducted on patterned graphene with widths in the range of 0.1–4  $\mu\text{m}$  which was grown by chemical vapour deposition and patterned by electron beam lithography. The microscopic behaviour of the Raman spectrum was investigated using image mapping from Raman spectroscopic data. Among three main peaks (D-band, G-band and 2D-band), the two-dimensional (2D) peak was clear even in 200 nm width graphene, however the D-band signal was very weak, confirming low defect concentration. It was found that the 2D-band line width was decreased as the width became narrower, which was explained by refining the electronic band structure because of confined sample size. The 2D- and G-band intensities were decreased by reducing the width because the laser beam spot size was greater than the width of the sample and the effective area generating the signal was reduced.

**1. Introduction:** Micropatterned graphene ribbons have attracted increasing attention because of the possibility of fabricating graphene-based nanoelectronics such as ultra high-speed field effect transistors or quantum dot devices. Raman spectroscopy has been used widely for graphene studies in terms of discerning the number of layers [1, 2], doping and disorder [3, 4], charged impurities [5], compression [6], heating effect [7], surface enhancement [8] and graphene size effect [9, 10]. Casiraghi *et al.* [11] measured Raman spectroscopy of graphene flakes with edges and analysed detailed Raman data changes at different crystallographic directions of graphene. A theory for Raman scattering was developed, and they explained the experimentally measured images of the disordered edges.

Bischoff *et al.* [10] measured the Raman spectra of the graphene nanoribbon in the range of 30–130 nm, fabricated from mechanically exfoliated graphene. They found that the absolute G- and 2D-band intensities scale with the nanoribbon width, whereas the D-band intensity depends only on the edge region of the nanoribbon including edge roughness. They concluded that the reactive ion etching (RIE) process used to pattern nanoribbon induced defects only at the edge but not inside the graphene nanostructures. In this Letter, we report Raman spectroscopic images of micropatterned graphene with different widths ranging from 100 nm to 4  $\mu\text{m}$ , fabricated from a chemical vapour deposition (CVD) grown graphene layer, to understand the effects of RIE in patterning process and limited size.

**2. Experimental details:** Graphene layers were grown by CVD technique on copper foil (25  $\mu\text{m}$  thick, 99.8% purity, Alfa Aesar, item no. 13382) at 950°C and at a pressure of  $-1 \times 10^{-3}$  Torr in a fused silica tube with 22 mm inner diameter. The Ar/H<sub>2</sub> mixture gas was flown at the rate of 250/100 SCCM (SCCM denotes cubic centimeter per minute at STP), and 50 SCCM of CH<sub>4</sub> was adopted as the carbon source in the CVD growing process. Fig. 1a shows the photographic image of the graphene sample deposited on copper foil by CVD.

To transfer the graphene deposited on Cu foil to a SiO<sub>2</sub>/Si wafer, polymethyl methacrylate (PMMA) (950, A2 from MicroChem Inc.) film was spin-coated (500 rpm for 5 s and 4000 rpm for 40 s) on top of the graphene layer. The Cu foil was dissolved in 1 M ammonium persulphate ((NH<sub>4</sub>)<sub>2</sub>S<sub>2</sub>O<sub>8</sub>) solution for one day and rinsed in deionised (DI) water. Standard-clean-2 (SC2) etching (20:1:1, 15 min at room temperature), DI water rinsing and SC1 etching

were performed sequentially to remove metallic and organic residues. The resulting graphene/PMMA layer was transferred upside-down onto Si/SiO<sub>2</sub> substrates and baked at 150°C for 15 min. The sample was dipped into acetone and IPA (isopropanol) to remove PMMA.

For the electron beam (e-beam) lithography, the same PMMA was again coated by a spinner on the sample as a resist. The spin-coating procedure was step1 (1000 rpm, 10 s) and step2 (5000 rpm, 30 s), and it was baked at 170°C for 10 min. The e-beam exposure dose was about 300  $\mu\text{C}/\text{cm}^2$  to make ribbon patterns, and the patterns were developed by MIBK (methyl isobutyl ketone) and IPA mixture with 1:3 ratio for 10 s. RIE was performed using O<sub>2</sub> plasma for 3 s to etch the graphene, and the sample was rinsed by acetone. Fig. 1b shows the sample photographic image after development, Fig. 1c after RIE and Fig. 1d after removing PMMA by acetone.

Raman scattering imaging was conducted using a microRaman system (Renishaw, InVia systems) with a laser line of 514.5 nm (argon ion) having 1800 grooves/mm grating and spectral resolution of  $-3 \text{ cm}^{-1}$ . The laser beam spot size was about 1  $\mu\text{m}$ , and the laser power was set to about 2 mW to prevent excessive

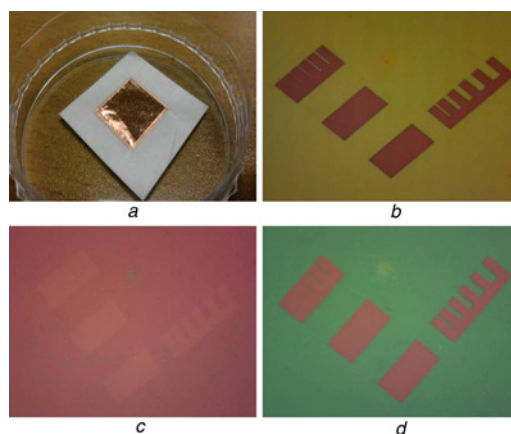


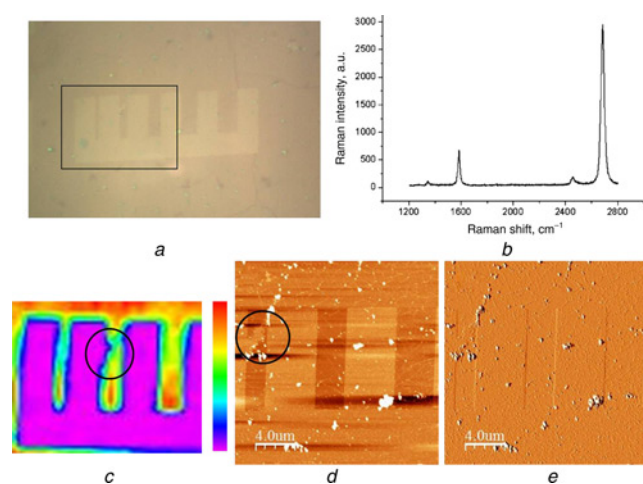
**Figure 1** Photographic image of representative graphene sample shown as deposited on piece of Cu foil (Fig. 1a). E-beam lithography was performed to fabricate the ribbon pattern. The optical microscopic images were taken after development (Fig. 1b), after RIE (Fig. 1c), and after removing PMMA by acetone finally (Fig. 1d)

heating on the samples. The Raman spectra were recorded while raster-scanning the sample with a piezo-stage scanner, and the spatial resolution was about 800 nm. The sample location was adjusted on a Raman sample stage by an optical microscope, and it was raster-scanned over the patterned area, taking point-by-point spectra. Topographic images were taken by an atomic force microscope (AFM) in non-contact mode with a cantilever having a resonance frequency of  $\sim 300$  kHz and force constant of  $\sim 50$  N/m.

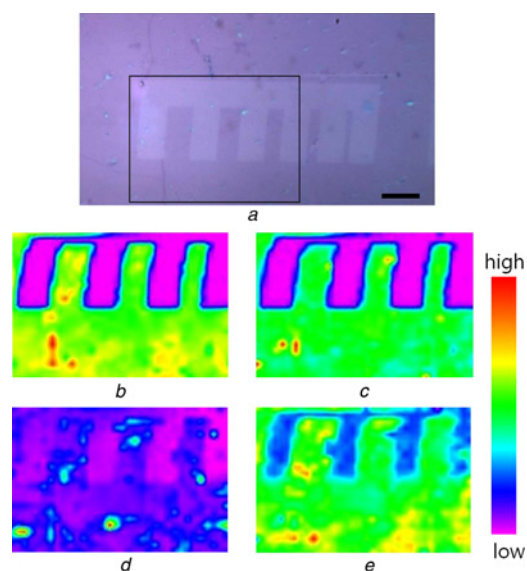
**3. Results and discussion:** The patterned graphene area indicated by a rectangle in Fig. 2a was investigated by a Raman spectrometer and AFM. From a Raman spectrum as shown in Fig. 2b, one can find three main peaks corresponding to the graphite structure at  $1350\text{ cm}^{-1}$  (D-band),  $1580\text{ cm}^{-1}$  (G-band) and  $2700\text{ cm}^{-1}$  (2D-band) [1]. The 2D-band peak is a typical peak having a single symmetric line shape representing a single-layer-graphene. The D-band peak near  $1350\text{ cm}^{-1}$  is not conspicuous, implying a ten small amount of defects on the graphene ribbon. The G-band comes from the  $E_{2g}$  phonon at the Brillouin zone centre, and the D-peak is due to the breathing modes of  $sp_2$  rings induced by defects, which is associated with intervalley electron scattering [1, 12–14].

From all spectra measured by raster scanning, the two-dimensional (2D) peak position was selected and the intensities were mapped in an image (Fig. 2c) following the colour code indicated by a right-hand colour bar. That is, the red part has the highest signal intensity of the 2D peak, and the purple area shows the lowest signal corresponding to the etched part, having no graphene layer. As a result, the intensity of the 2D peak was changed depending on the ribbon widths and locations. It is noticeable that the second and third ribbons' widths (2 and  $3\text{ }\mu\text{m}$ , respectively) were larger than the Raman laser beam spot, but the mapping image shows the width dependence of the ribbons. The part indicated by a circle has irregular boundary shape because of defective etching by dirt particles, which was confirmed by the AFM measurements, as shown in the Fig. 2d topographic and the Fig. 2e error images. The AFM images show some dirt, which is suspectedly because of residues resulting from the CVD growing or transfer process. It is well known that the PMMA residue after graphene transfer can hardly be removed completely [15, 16].

From the optical microscopic image of the sample in Fig. 3a, the other patterned area was selected and the Raman spectrum for each point was measured. The Raman data were reorganised into intensity mapping for each band and their ratio. The 2D-band mapping



**Figure 2** Optical microscopic image, patterned part was selected (Fig. 2a); representative spectrum of Raman data (Fig. 2b); mapped 2D-band peak intensity (Fig. 2c), which was compared with topographic image (Fig. 2d) and error image (Fig. 2e) taken by non-contact mode AFM



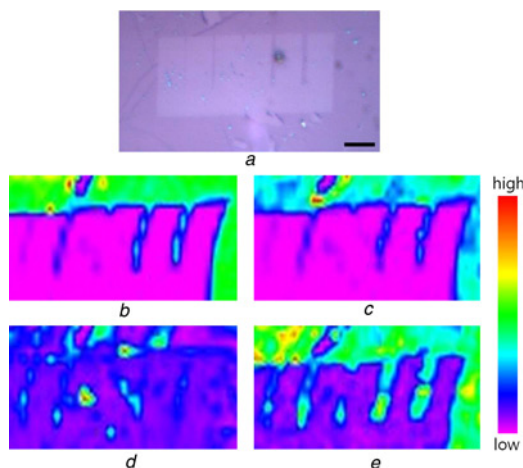
**Figure 3** Optical microscopic image of sample (Fig. 3a). Micropatterned graphene ribbons with widths of 4, 3 and  $2\text{ }\mu\text{m}$ , from left to right are shown in optical microscopic image (scale bar =  $5\text{ }\mu\text{m}$ ) Raman mapping images of 2D-band peak intensity (Fig. 3b), G-band peak intensity (Fig. 3c), D-band peak intensity (Fig. 3d),  $I(2D)/I(G)$  ratio were taken simultaneously (Fig. 3e)

image shows high intensity in the middle of the ribbons with widths 4, 3 and  $2\text{ }\mu\text{m}$  which is almost the same as the unpatterned area (lower part). Some parts have exceptionally higher intensity of the 2D-peak, because of the non-uniformity of the sample. The edges of the ribbons show lower intensity because they are covered partially by the laser beam. This effect is very natural and already reported by another group [10]. The G-band Raman mapping image also shows similar behaviour, as shown in Fig. 3c. Three different size ribbons have similar intensities, and only edges have lower intensities, in both cases of 2D-band and G-band.

On the other hand, the D-peak intensity depends on the amount of disorder, generally [11]. Owing to good sample quality, the D-band map in Fig. 3d shows a blurred image. At the edges of the patterned-graphene many defects could be induced by ion irradiation in the RIE process and a significant intensity in the Raman D-band peak was expected, but our result shows that D-band intensity was not enhanced at the edge. According to Casiraghi *et al.*, when going from outside to inside the flake, the D-peak intensity increased, reached a maximum and then decreased because the defects were mainly located at the edge [11]. However, our result implies that the sample was not damaged by ion irradiation.

The intensity ratios between the Raman bands were mapped. As the intensity of 2D-band,  $I(2D)$ , decreased moving to the outside because the allowed signal was proportional to the volume of the sample, the same was observed for the intensity of G-band,  $I(G)$ . Therefore the ratio  $I(2D)/I(G)$  does not show any singular behaviour, except some spots having strong intensity of the peaks, as shown in Fig. 3e. In the case of D-band, the intensity was too weak to be analysed by mapping the ratios with credibility. As a result, each band's Raman peak intensity was not affected by the finite size in this scale.

The narrower graphene nanoribbons (100, 200, 300, 400 and  $500\text{ nm}$ ) were intended to be fabricated, but the  $300\text{ nm}$  ribbon was not well developed as shown in Fig. 4a. The Raman mapping data of peaks were measured as shown in Fig. 4b  $I(2D)$ , Fig. 4c  $I(G)$ , Fig. 4d  $I(D)$  and Fig. 4e  $I(2D)/I(G)$  ratio. Raman mapping images were expected to be similar to the results for the wider ribbons, but the images show contrast corresponding to the



**Figure 4** Graphene nanoribbons with different widths 100, 200, 300, 400 and 500 nm were fabricated, as shown in Figs. 4a–e. Optical microscopic image (Fig. 4a) (scale bar = 5  $\mu\text{m}$ ) Raman mapping images of 2D-band peak intensity (Fig. 4b), G-band peak intensity (Fig. 4c), D-band peak intensity (Fig. 4d),  $I(2D)/I(G)$  ratio are shown together (Fig. 4e)

edge of the wider ribbons. All things considered,  $I(2D)$  and  $I(G)$  are roughly proportional to the widths of the ribbons. Thus, we can infer that the intensity was proportional to the sampling area since the beam size was larger than the ribbon. The image of  $I(D)$  was much blurred, confirming that the nanoribbons do not have significant defects. In general, as crystalline grains or inter-defect distance grows in graphene, the ratio,  $I(D)/I(G)$ , varies inversely [11], but our data cannot be analysed in terms of this argument because of the low intensity of the D-band.

The intensity of the 2D-band was still strong on the ribbons with widths greater than 200 nm, and the shapes in the  $I(2D)/I(G)$  map were clear which means that the ribbons were not damaged in the RIE process. According to Casiraghi *et al.* [3], the intensity of the G-peak was not strongly affected by the small amount of doping or disorder, but the intensity of the 2D-peak strongly decreased with increasing doping or disorder. However, our result is not in agreement with theirs. Even the relative intensity of 2D-band to G-band became clear compared with the surrounding background.

The trend of the peaks' intensity and shape was analysed according to ribbon width, as shown in Fig. 5. From four sets of independent samples with different ribbon widths, the  $I(2D)/I(G)$  data were taken in Fig. 5a. They are in the range of 1.6–2.4, which are the typical values for single-layer-graphene [1]. Some data show the increasing trend of  $I(2D)/I(G)$  as the width was narrower, but not always. Considering the average data quality and accuracy, the size effect of the Raman peak intensities was not noticeable. Fig. 5b shows the full-width-of-half-maximum (FWHM) of G-band peak against ribbon width. Depending on the sample, the trend was varied, which is considered as a random behaviour because of experimental error.

However, the FWHM of the 2D-band peak against ribbon width has a consistent trend as shown in Fig. 5c for all the samples. The 2D-band is the second-order effect of the D-band, and it has a single narrow peak in single layer graphene (SLG), whereas it splits into four peaks in bilayer graphene because of evolution of the band structure [1]. In general, the width of the 2D-peak could be related with the number of layers, but our sample is single-layer and the ribbon patterning cannot change the number of layers. For SLG, the position of the 2D-band peak is determined by a double resonance process, where the phonon wave vectors are coupled with the electronic band structure [1]. The double resonance process is a fourth-order process involving four virtual transitions as shown in Fig. 5d: (i) excitation of electron–hole pair by

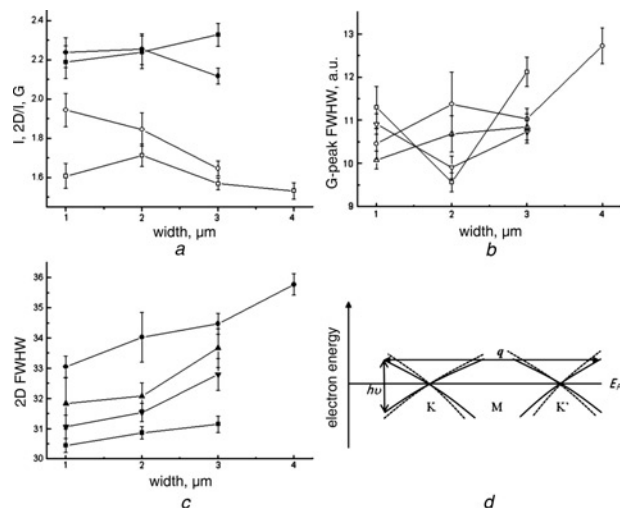


**Figure 5** Fig. 5a: ratio of 2D-peak and G-peak intensity plotted against graphene ribbon width, for four independent samples. Fig. 5b: FWHM of G-band peak. Fig. 5c: 2D-band peak plotted against ribbon widths. Each data point was taken from averaging all the measured values at the corresponding ribbon parts (the lines connect the set of data taken from ribbons fabricated in the same wafer). Fig. 5d: diagram shows relationship between electronic band structure and 2D-band peak width

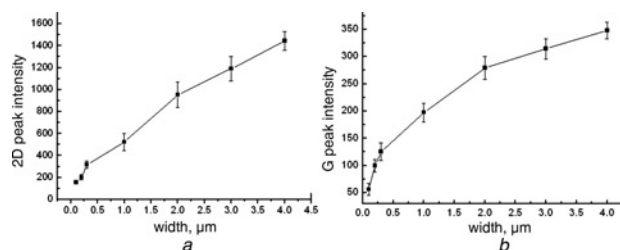


**Figure 6** From Raman spectroscopic data of graphene ribbons: the intensities of 2D-peak (Fig. 6a) and G-peak (Fig. 6b) plotted against width (each data point calculated by averaging values extracted from ribbon area)

photon energy ( $h\nu$ ) causing vertical transition, (ii) electron–phonon scattering with an exchanged momentum  $q$  close to K-point, (iii) electron–phonon scattering with an exchanged momentum  $-q$  close to K'-point and (iv) electron–hole recombination. The Raman frequency in this process is determined by the scattering phonon with  $q$ . If the sample has disorders and the band structure has perturbation (dashed lines) because of impurities and defects, then the momentum  $q$  has variation and the 2D-band peak width is broadened. As a result, because of the decrease of 2D-bandwidth we can infer that the finite size of the graphene ribbon decreased variation of the impurities and the band structures became uniform.

Fig. 6 shows the evolution of peak intensities against ribbon width, where the samples were prepared in different widths in the range of 0.1–4  $\mu\text{m}$ . They show the decreasing behaviour of 2D- and G-band peak intensities as the ribbon becomes narrower, consistently. Moreover, the two band peaks are in the same trend although their scattering mechanisms are quite different. As mentioned above, this behaviour can be explained by the Raman intensity of the allowed signal being proportional to the volume of the sample. Therefore it is not the size effect of the intrinsic property of graphene. It is because of the resolution limit of microRaman equipment in terms of instrumentation.

**4. Conclusion:** The CVD grown graphene was patterned by e-beam lithography in ribbon shape with widths in the range of 0.1–4  $\mu\text{m}$ . The Raman spectroscopic image resolved the

nanoribbon even with 100 nm width. From the spectra, three main graphite peaks were extracted and mapped into 2D images. The 2D-peak was clear even with 200 nm width, however the D-band signal was weak even at the edge of the ribbon, confirming that the sample was high quality, having low defect or rarely being damaged by RIE etching. The decrement of the 2D-band line width by narrowing the ribbon width meant that confining sample size reduced the variation of disorder and caused the electronic band structure to be homogeneous. The 2D- and G-band intensities were decreased by narrowing the width of the ribbon because the effective area generating the signal was reduced.

**5. Acknowledgments:** This research was supported by the Basic Science Research Program (2009-0070725, 2010-0005393 and 2012R1A6A1029029), and the Priority Research Centers Program (2012-0005859) through NRF funded by MEST.

## 6 References

- [1] Ferrari A.C., Meyer J.C., Scardaci V., *ET AL.*: 'Raman spectrum of graphene and graphene layers', *Phys. Rev. Lett.*, 2006, **97**, (18), p. 187401
- [2] Gupta A., Chen G., Joshi P., Tadigadapa S., Eklund P.C.: 'Raman scattering from high-frequency phonons in supported N-graphene layer films', *Nano Lett.*, 2006, **6**, (12), pp. 2667–2673
- [3] Casiraghi C.: 'Raman intensity of graphene', *Phys. Status Solidi B*, 2011, **248**, pp. 2593–2597
- [4] Basko D.M.: 'Theory of resonant multiphonon Raman scattering in graphene', *Phys. Rev. B*, 2008, **78**, p. 125418
- [5] Ni Z.H., Yu T., Luo Z.Q., *ET AL.*: 'Probing charged impurities in suspended graphene using Raman spectroscopy', *ACS Nano*, 2009, **3**, (3), pp. 569–574
- [6] Chen C.C., Bao W., Theiss J., Dames C., Lau C.N., Cronin S.B.: 'Raman spectroscopy of ripple formation in suspended graphene', *Nano Lett.*, 2009, **9**, (12), pp. 4172–4176
- [7] Ioffe Z., Shamai T., Ophir A., *ET AL.*: 'Detection of heating in current-carrying molecular junctions by Raman scattering', *Nature Nanotechnol.*, 2008, **3**, (12), pp. 727–732
- [8] Pan S.G., Liu X.H., Wang X.: 'Preparation of Ag<sub>2</sub>S-graphene nanocomposite from a single source precursor and its surface-enhanced Raman scattering and photoluminescent activity', *Mater. Charact.*, 2011, **62**, (11), pp. 1094–1101
- [9] Ryu S., Maultzsch J., Han M.Y., Kim P., Brus L.E.: 'Raman spectroscopy of lithographically patterned graphene nanoribbons', *ACS Nano*, 2011, **5**, (5), pp. 4123–4130
- [10] Bischoff D., Güttinger J., Dröscher S., Ihn T., Ensslin K., Stampfer C.: 'Raman spectroscopy on etched graphene nanoribbons', *J. Appl. Phys.*, 2011, **109**, p. 073710
- [11] Casiraghi C., Hartschuh A., Qian H., *ET AL.*: 'Raman spectroscopy of graphene edges', *Nano Lett.*, 2009, **9**, (4), pp. 1433–1441
- [12] Thomsen C., Reich S.: 'Double resonant Raman scattering in graphite', *Phys. Rev. Lett.*, 2000, **85**, (24), pp. 5214–5217
- [13] Narula R., Reich S.: 'Double resonant Raman spectra in graphene and graphite: a two-dimensional explanation of the Raman amplitude', *Phys. Rev. B*, 2008, **78**, p. 165422
- [14] Chen J.H., Cullen W.G., Jang C., Fuhrer M.S., Williams E.D.: 'Defect scattering in graphene', *Phys. Rev. Lett.*, 2009, **102**, (23), p. 236805
- [15] Pirkle A., Chan J., Venugopal A., *ET AL.*: 'The effect of chemical residues on the physical and electrical properties of chemical vapor deposited graphene transferred to SiO<sub>2</sub>', *Appl. Phys. Lett.*, 2011, **99**, (12), p. 122108
- [16] Lin Y.-C., Lu C.-C., Yeh C.-H., Jin C., Suenaga K., Chiu P.-W.: 'Graphene annealing: how clean can it be?', *Nano Lett.*, 2012, **12**, pp. 414–419